



**HAL**  
open science

## On The Use of Nonlinear Receding-Horizon Observers in Batch Terpolymerization Processes

Mazen Alamir, Nida Sheibat-Othman, Sami Othman

► **To cite this version:**

Mazen Alamir, Nida Sheibat-Othman, Sami Othman. On The Use of Nonlinear Receding-Horizon Observers in Batch Terpolymerization Processes. NOLCOS 2007 - 7th IFAC Symposium on Nonlinear Control Systems, Aug 2007, Petroria, South Africa. 10.3182/20070822-3-ZA-2920.00123 . hal-00116962

**HAL Id: hal-00116962**

**<https://hal.science/hal-00116962>**

Submitted on 13 Dec 2006

**HAL** is a multi-disciplinary open access archive for the deposit and dissemination of scientific research documents, whether they are published or not. The documents may come from teaching and research institutions in France or abroad, or from public or private research centers.

L'archive ouverte pluridisciplinaire **HAL**, est destinée au dépôt et à la diffusion de documents scientifiques de niveau recherche, publiés ou non, émanant des établissements d'enseignement et de recherche français ou étrangers, des laboratoires publics ou privés.

# On The Use of Nonlinear Receding-Horizon Observers in Batch Terpolymerization Processes

Mazen Alamir\*

Laboratoire d'Automatique de Grenoble (LAG),

CNRS-University of Grenoble, France.

E-mail: mazen.alamir@inpg.fr

\*Corresponding author

Nida Sheibat-Othman and Sami Othman

Laboratoire d'Automatique et de Génie des Procédés (LAGEP),

UCBL/CNRS -ESCPE Bât. 308G 43, Bd du 11 Nov. 1918

69622 Villeurbanne Cedex, France,

Email: nida.othman@lagep.cpe.fr, sami.othman@lagep.cpe.fr

**Abstract:** In this paper, a nonlinear receding-horizon observer is proposed for state reconstruction in batch terpolymerization reactors. The related investigations show that the state reconstruction problem may be quite ill conditioned in the sense that different states may exist that lead to roughly the same output. It seems however that when constrained receding-horizon estimation is used together with a dedicated crossing singularity heuristic, state reconstruction is possible even in presence of measurement noise and up-to 10% error on the r.h.s of the ODE's describing the system's dynamics. The efficiency and the real-time implementability of the overall scheme is shown through illustrative scenarios including both simulation and experimental validation.

**Keywords:** Nonlinear Constrained State Estimation; Batch Terpolymerization Reactor; Crossing Singularity Oriented Heuristic; Experimental Results; Robust Estimation.

---

## 1 INTRODUCTION

---

Multimonomer systems are usually used to produce polymeric materials with suitable final properties. Terpolymerization systems usually allow producing high performance materials. In order to control the final polymer properties, such as the polymer composition, it is of high importance to model and monitor such processes. In this work, we will be interested in estimating the polymer composition in emulsion terpolymerization. The heterogeneity of emulsion polymerizations makes it difficult to monitor the concentration of monomer online especially with the number of monomers involved in the reaction. Urretabizkain et al. (1994) used an online gas chromatographe to measure the residual amounts of monomer in emulsion terpolymerization. The authors outlined some difficulties due to the process heterogeneity and inaccuracy of results in the presence of monomer droplets.

Different estimation methods have been used to mon-

itor polymerization processes. The most widely used method is still the Extended Kalman filter (see for instance Dimitrators et al. (1989), Kozub and Macgregor (1992), Wang et al. (1995), Scali et al. (1997), Kiparisides et al. (2002)) but different applications of nonlinear techniques can nowadays be found (Hammouri et al. (1999), Dootingh et al. (1992), Soroush (1997), Tatiraju et al. (1999) and Alvarez and Lopez (1999)). Recently, sliding-mode observers were used by BenAmor et al. (2004) and Aguilar-Lopez and Maya-Yescas (2005) to estimate the monomer concentration and average molecular weight in solution homopolymerization.

While several estimators have been proposed for polymerization processes, as long as emulsion terpolymerization is concerned, only two applications could be found in the literature. Buruaga et al. (2000) constructed an open loop observer to estimate the

Copyright © 200x Inderscience Enterprises Ltd.

polymer composition using calorimetric measurements combined to the process model. The authors outlined however that the polymerization rate of each monomer is not observable from the overall heat of the reaction. Othman et al. (2001) constructed a closed loop high gain observer to estimate the polymer composition and showed by simulation and experimentally that the system can be observable if the total amounts of monomers are measured. However, because of the model complexity (see section 2), the design of such a high gain observer and the tuning its gain in order to cope with the system constraints remains a quite involved task and the observer so obtained is highly dependent on the structure of the model.

In this work, a receding horizon observer is used to estimate the individual amounts of monomer in the reactor as well as the number of moles of radicals in the polymer ( $\mu$ ) using the overall monomer conversion that can be obtained by calorimetry. The paper is organized as follows: First, the process model is presented (section 2). Then, a brief presentation of the receding-horizon observer algorithm is proposed (section 3) with a discussion on some numerical issues and the associated solutions. In particular a singularity-cross oriented heuristic is proposed and its efficiency is shown. The observer is then applied to the terpolymerization process (section 4). First the robustness of the proposed observer against model uncertainties is shown by simulating up to 10% random error on the r.h.s of the system's equation in the presence of measurement noise (section 4.1). Then the observer is validated experimentally (section 4.2) during the emulsion terpolymerization of butyl acrylate, methyl methacrylate and vinyl acetate. In all cases, the real-time implementability of the proposed observer is assessed under 30 seconds sampling time assumption.

## 2 Modelling

Assuming that monomers are not soluble in the aqueous phase and that the reaction takes place mainly in the polymer particles, the material balances of monomers are given by:

$$\dot{N}_i = Q_i - R_{P_i} \quad i = 1, 2, 3 \quad (1)$$

The reaction rate in the polymer particles  $R_{P_i}$  is proportional to the concentration of monomer in the polymer particles ( $[M_i^P]$ ) and the number of moles of radicals in the polymer particles ( $\mu$ ):

$$R_{P_i} = \mu [M_i^P] (k_{p1i} P_1^P + k_{p2i} P_2^P + k_{p3i} P_3^P) \quad (2)$$

The time averaged probabilities ( $P_i^P$ ) that an active

chain be of ultimate unit of type  $i$  are defined by:

$$\begin{aligned} P_1^P &= \frac{\alpha}{\alpha + \beta + \gamma} \\ P_2^P &= \frac{\beta}{\alpha + \beta + \gamma} \\ P_3^P &= 1 - P_1^P - P_2^P \end{aligned} \quad (3)$$

where

$$\begin{aligned} \alpha &= [M_1^P] (k_{p21} k_{p31} [M_1^P] + k_{p21} k_{p32} [M_2^P] + k_{p31} k_{p23} [M_3^P]) \\ \beta &= [M_2^P] (k_{p12} k_{p31} [M_1^P] + k_{p12} k_{p32} [M_2^P] + k_{p13} k_{p32} [M_3^P]) \\ \gamma &= [M_3^P] (k_{p13} k_{p21} [M_1^P] + k_{p21} k_{p23} [M_2^P] + k_{p13} k_{p23} [M_3^P]) \end{aligned}$$

In emulsion polymerization, it is well known that the reaction can be divided into three intervals. In interval I, the polymer particles are produced. Modelling of this interval allows the calculation of the particle size distribution and the average number of radicals per particle which allows to calculate the total number of moles of radicals in the polymer particles ( $\mu$ ) in equation 2. This part of the model will not be considered since it adds a lot of complexity to the process model besides the fact that it remains very sensitive to impurities.  $\mu$  will therefore be considered as a parameter in the process model to be estimated without modelling. It is important to outline that  $\mu$  can undergo important changes during the reaction since it is affected by the gel effect phenomena.

In interval II, the particle number is supposed to be constant. Polymer particles are saturated with monomer and the excess of monomer is stored in the monomer droplets. During interval III, monomer droplets disappear and all the residual monomer is supposed to be in the polymer particles. Therefore, the concentration of monomer in the polymer particles can be calculated by the following system:

$$[M_i^P] = \begin{cases} \frac{(1 - \phi_p^P) N_i}{\sum_j \frac{N_j MW_j}{\rho_j}}, & II \\ \frac{N_i}{\sum_j MW_j \left( \frac{N_j^T - N_j}{\rho_{j,h}} + \frac{N_j}{\rho_j} \right)}, & III \end{cases} \quad (4)$$

The condition for the existence of monomer droplets and therefore for determining if the reaction is in interval II, is governed by the following equation:

$$N_1 \delta_1 + N_2 \delta_2 + N_3 \delta_3 - \frac{(1 - \phi_p^P)}{\phi_p^P} \sigma > 0 \quad (5)$$

where

$$\delta_i = MW_i \left( \frac{1}{\rho_i} + \frac{(1 - \phi_p^P)}{\rho_{i,h} \phi_p^P} \right), \quad i = 1, 2, 3 \quad (6)$$

and

$$\sigma = \sum_{j=1}^3 \frac{MW_j N_j^T}{\rho_j, h} \quad (7)$$

The overall monomer conversion that can be measured easily online by calorimetry is defined by:

$$y = \frac{\sum_{i=1}^3 MW_i (N_i^T - N_i)}{\sum_{j=1}^3 MW_j N_j^T} \quad (8)$$

Parameters used for the experimental validation of the model are given in table 1 where  $k_{pij} = k_{pii}/r_{ij}$ .

Parameter	Value	Unit
$\phi_p^p$	0.4	
$MW_1$	128.2	(g/mol)
$MW_2$	100.12	(g/mol)
$MW_3$	86.09	(g/mol)
$\rho_1$	0.89	(g/cm <sup>3</sup> )
$\rho_2$	0.94	(g/cm <sup>3</sup> )
$\rho_3$	0.93	(g/cm <sup>3</sup> )
$\rho_{1,h}$	1.08	(g/cm <sup>3</sup> )
$\rho_{2,h}$	1.15	(g/cm <sup>3</sup> )
$\rho_{3,h}$	1.17	(g/cm <sup>3</sup> )
$k_{p11}$	$4.5 \times 10^5$	(cm <sup>3</sup> /mol/s)
$k_{p22}$	$1.28 \times 10^6$	(cm <sup>3</sup> /mol/s)
$k_{p33}$	$4.26 \times 10^6$	(cm <sup>3</sup> /mol/s)
$r_{12}$	0.355	
$r_{21}$	1.98	
$r_{13}$	6.635	
$r_{31}$	0.037	
$r_{23}$	22.21	
$r_{32}$	0.07	

Table 1: Parameter values of the terpolymerization of BuA/MMA/VAc (used in the experimental validation)

The recipe used for the experimental validation of the observer is given by table 2 Othman et al. (2001).

Component	Charge (g)
Butyl acrylate	300
Methyl methacrylate	300
Vinyl acetate	60
Sodium dioctyl sulfosuccinate	3
Potassium persulfate	2
Water	2380

Table 2: Recipe of the terpolymerization of BuA/MMA/VAc

### 3 The Nonlinear Receding-Horizon Observer

Consider a nonlinear system described by the following set of ODE's

$$\dot{x} = f(x, u) \quad ; \quad y = h(x) \quad (9)$$

where  $x \in \mathbb{R}^n$  stands for the state vector,  $u \in \mathbb{R}^{n_u}$  a vector of exogenous input and  $y \in \mathbb{R}^{n_y}$  is the vector of measured outputs. The state estimation problem amounts to use the output measurement in order to retrieve the value of the state vector  $x$ .

In this paper, it is assumed that some sampling period  $\tau_s > 0$  is used to update the computations leading to sampling instants  $t_k = k\tau_s$  with  $k \in \mathbb{N}$ . It is also assumed that the measures are acquired using the same sampling rate.

In the remainder of the paper, the notation

$$X^{(k+)}(i, x, u(\cdot)) \quad ; \quad i \geq k$$

denotes the forward solution of (9) at instant  $i\tau_s$  starting from state  $x$  at instant  $k\tau_s$  under the input profile  $u(\cdot)$ . Similarly, the notation

$$X^{(k-)}(i, x, u(\cdot)) \quad ; \quad i \leq k$$

is used for backward integration.

Receding-Horizon observers (Michalska and Mayne, 1995) produce an estimation  $\hat{x}(t_k)$  of the true state  $x(t_k)$  by minimizing the output prediction error over some past time horizon, namely for all  $k \geq N_p^{min}$ , the estimation  $\hat{x}(t_k)$  is given by:

$$\hat{x}(t_k) = \arg \min_{\xi \in \mathcal{X}(t_k)} J(t_k, \xi, y(\cdot), u(\cdot)) := \sum_{i=k-N_p(k)}^k \|y(i\tau_s) - h(X^{(k-)}(i, \xi, u(\cdot)))\|_{Q_i}^2 \quad (10)$$

where

- ✓ The estimation horizon  $N_p(k)$  is chosen such that:

$$N_p(k) = \begin{cases} N_p^{max} & \text{if } k \geq N_p^{max} \\ k & \text{if } N_p^{min} \leq k \leq N_p^{max} \end{cases} \quad (11)$$

Namely, no optimization-based estimation is made before at least  $N_p^{min}$  measurements are available. More precisely, for  $k < N_p^{min}$ , an open-loop model based updating scheme is used according to

$$\hat{x}(t_k) = X^{((k-1)+)}(k, \hat{x}(t_{k-1}), u(\cdot)) \quad (12)$$

Note that the horizon length does not exceed  $N_p^{max}$  since too early measurement may probably be irrelevant due to modelling errors and/or the occurrence of exogenous unmeasured disturbances .

- ✓ The subset  $\mathcal{X}(t_k) \subset \mathbb{R}^n$  is the subset of admissible values of the state at instant  $t_k$ . This enables to handle constraints on the state that is of great interest in bio-processes state estimation. Typically, the state components  $N_i$  as well as  $\mu$  must remain positive and in the particular case of the batch reactor under interest, their values cannot exceed the initial values  $N_i^T$  plus an amount that may reflect an upper bound on the initial estimation error.
- ✓  $Q_i$  are positive definite weighting matrices that may depend on  $i$  either to induce a *forgetting* behavior or to enhance local minima avoidance capacity (see section 3.1 hereafter)

**Remark 1.** Note that quite often, receding-horizon state estimation is formulated as an optimization problem in the unknown  $z(t_k) := \hat{x}(t_k - N_p \tau_s)$ . The estimated state at instant  $t_k$  is then obtained by forward integration of the system model:

$$\hat{x}(t_k) = X^{(k-N_p)^+}(k, z(t_k), u(\cdot))$$

This lead to computation in which only forward integrations are used. As a matter of fact, in the absence of modelling errors, the two estimation schemes are equivalent. However, when the model used by the observer differs from the real one, the backward-forward scheme adopted in this paper is more robust. ♠

The optimization problem (10) is generally a constrained non convex and its solution has to be obtained through iterative schemes. Considering the discontinuities in the r.h.s of the terpolymerization process model, the Downhill simplex algorithm (Press et al., 1992) is used in this paper since it requires no gradient computations. The modified Direction Set Powell's algorithm (Press et al., 1992) that shares this nice property has also been tested with almost similar results.

Regardless the iterative scheme being used, its concrete use for on-line state estimation purpose involves the definition of a maximum number of *function evaluations*, say  $N_{FE} \in \mathbb{N}$  together with a stopping threshold on the cost function variations  $\varepsilon > 0$ . Therefore, receding-horizon state estimation can be shortly denoted as follows:

$$\hat{x}(t_k) = I_\varepsilon^{N_{FE}} \left( t_k, \hat{x}^+(t_{k-1}), y(\cdot), u(\cdot) \right) \quad (13)$$

where the r.h.s of (13) is the value of the decision variable  $\xi$  that gives the best achieved value of the cost function (10) by the iterative process under the upper bound  $N_{FE}$  on the number of function evaluations when using the stopping threshold  $\varepsilon$  and starting with the initial guess  $x^+(t_{k-1})$  that is computed using the last state estimate by one step forward integration, namely

$$\hat{x}^+(t_k) = X^{(k-1)^+}(k, \hat{x}(t_{k-1}), y(\cdot), u(\cdot)) \quad (14)$$

that is used as an initial guess in the iterative process (13) (the downhill simplex, powell's method or whatsoever).

### 3.1 Numerically indistinguishable states / local minima

When looking for a solution to the optimization problem (10), the iterative process (13) may encounter two problems:

- ✓ *The presence of numerically indistinguishable states*  
This arises when at some instant  $t_k$ , the iteration reaches some state  $\xi \neq x(t_k)$  for which

$$J(t_k, \xi, y(\cdot), u(\cdot)) \approx J(t_k, x(t_k), y(\cdot), u(\cdot)) \approx 0$$

where approximate equality are related to the threshold  $\varepsilon$  that is used in (13). Note that the possibility to face this situation is related to the fundamental issue of observability and cannot be avoided by any algorithmic tricks. However, the use of state constraints may isolate indistinguishable states that are physically irrelevant. This is one of the advantages in using optimization based observer.

- ✓ The presence of local minima that does not necessarily correspond to a low value of the cost function.

This second problem is an unavoidable issue in nonconvex optimization that is generally afforded by multiple starting points approach when no other characterization of the global minimum is available. Fortunately, when dealing with state estimation problem, the global minimum  $x(t_k)$  one looks for when trying to solve the optimization problem (10) can be strongly characterized by the following property:

$x(t_k)$  is a global minimum of (10) **for any** sequence of positive definite weighting matrices  $Q_i$ .

This makes *the state estimation problem* a very particular optimization problem since the global minimum one is looking for is THE global minimum of an infinite number of known functions. A subset of this set of functions sharing  $x(t_k)$  as global minimum can be generated by choosing

$$Q_i = \gamma^i \cdot q_i \cdot \mathbb{I}_{n_y} \quad \text{s.t.} \quad q_i > 0 \quad \text{and} \quad \sum_i q_i = 1 \quad (15)$$

where  $\gamma \in ]0, 1[$  is the forgetting factor while  $\mathbb{I}_{n_y}$  stands for the identity matrix in  $\mathbb{R}^{n_y \times n_y}$ .

Note that since the vector of weights

$$\bar{q} := (q_1 \quad q_2 \quad \dots)^T$$

is involved in the definition of the cost function (10), the iterative process (13) can be worth written as follows

$$\hat{x}(t_k) = I_{\varepsilon, \bar{q}}^{N_{FE}} \left( t_k, \hat{x}^+(t_{k-1}), y(\cdot), u(\cdot) \right) \quad (16)$$

The idea is then to notice that a local minimum for (10) in which some weighting vector  $\bar{q}^{(1)}$  is used may

probably not remain a local minimum for another randomly chosen value of  $\bar{q}^{(2)}$  since it seems reasonable to admit that only the true state  $x(t_k)$  is a singular point for all possible values of the weighting vector  $\bar{q}$ .

Following this intuition, the *one trials* updating rule (16) is replaced by the following *multiple trials* updating rule:

---

```

 $\bar{q} \leftarrow \frac{1}{N_p} (1 \ 1 \ \dots)^T$ 
 $x_{guess} \leftarrow \hat{x}^+(t_{k-1})$  [see (14)]
for ( $i = 1 : N_{\text{trials}}$ )
     $x_{guess} \leftarrow I_{\varepsilon, \bar{q}}^{N_{FE}}(t_k, x_{guess}, y(\cdot), u(\cdot))$ 
    Generate randomly new  $\bar{q}$  satisfying (15).
end
 $\hat{x}(t_k) \leftarrow x_{guess}$ 

```

---

Note that when  $N_{\text{trial}} = 1$ , the last *multiple trials* updating rule gives the classical iteration (13). Note also that the above updating rule takes  $\hat{x}(t_{k-1})$ ,  $y(\cdot)$  and  $u(\cdot)$  as inputs and delivers the updated estimation  $\hat{x}(t_k)$  as output yielding a dynamic state observer.

---

#### 4 Application to terpolymerization processes

---

In this section, the receding horizon observer strategy proposed in section 3 is used to reconstruct the state of the batch terpolymerization process. In this section, both simulation and experimental results are proposed. Indeed:

- ✓ Simulations enable various model uncertainties as well as measurement noise to be tested and the behavior of the proposed state observer can be investigated.
- ✓ Experimental results allow to check the quality of the pair (model+observer) in the sense that there is no more a *true model* to which modeling error assumptions are associated, but we only have true measurements and an estimation scheme based on the system model. This validation is the ultimate one in the sense that it involves both the quality of the model and the associated estimation scheme and answers the only *interesting question* on whether the proposed solution (model+observer) enables to reconstruct the state of the system as well as the value of  $\mu$  despite its unknown dynamic.

In order to apply the receding-horizon estimation scheme proposed in the preceding section to reconstruct the value of  $N := (N_1, N_2, N_3)$  and  $\mu$ , a constant evolution of  $\mu$  is assumed (over the prediction horizon) and the general state equation (9) is built up with the state vector being defined by :

$$x := (N_1 \ N_2 \ N_3 \ \mu) \in \mathbb{R}_+^4 \quad ; \quad \dot{\mu} = 0$$

Recall however that despite this constant behavior during the prediction horizon, the resulted *closed-loop* estimation of  $\mu$  may show dynamic behavior thanks to the moving horizon technique (see figures 6 and 7).

Considering global relative uncertainties  $d_1, d_2$  and  $d_3$ , the following model is obtained to be used by the observer:

$$\dot{N} = \begin{pmatrix} 1 + d_1 & 0 & 0 \\ 0 & 1 + d_2 & 0 \\ 0 & 0 & 1 + d_3 \end{pmatrix} \cdot f(x, u) \quad (17)$$

$$\dot{\mu} = 0 \quad (18)$$

$$y = (1 + \nu) \cdot h(x) \quad (19)$$

Namely, relative uncertainties are introduced directly on the r.h.s of the system ODE's through the variables  $d_i$ 's. This can gather all sources of model discrepancy. On the other hand measurement noises are introduced through the variable  $\nu$  used in the measurement equation (19).

#### 4.1 Simulation results

This section successively illustrates the following points:

- ◇ **The unconstrained state estimation problem of the terpolymerization process may be ill-conditioned.** This is shown on figure 1 where it can be noticed that roughly the same output can be obtained for two quite different state vectors.

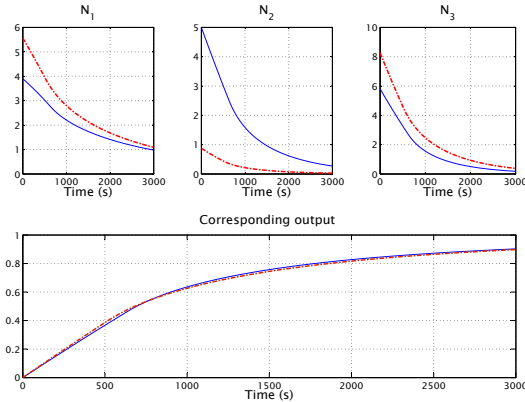


Figure 1: *Illustration of an ill conditioned estimation problem. Two quite different initial values of  $(N_1, N_2, N_3)$  lead to almost the same output.*

- ◇ **The Receding-Horizon state estimation is robust against measurement noise and model uncertainties**

In order to check the robustness of the state estimation scheme, the values of the  $d_i$ 's and  $\nu$  are updated every sampling period from a uniform random distribution according to

$$d_i(k) = d_{max} \cdot r_i(k) \quad (20)$$

$$\nu(k) = \nu_{max} \cdot r_\nu(k) \quad (21)$$

where the  $r_i(k)$ 's and  $\nu(k)$  are chosen randomly in  $[0, 1]$ . The results are shown on figures 2 and 3 (respectively without and in the presence of measurement noises) where up to 10% relative errors are introduced on the r.h.s of the system's model.

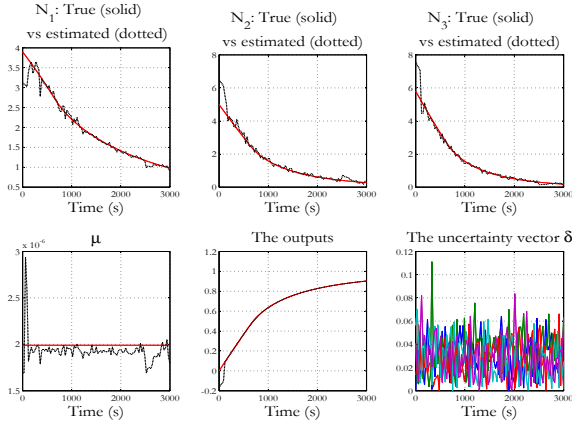


Figure 2: Observer behavior under model uncertainty given by (17)-(21) with  $d_{max} = 10\%$  and no measurement noise ( $\nu_{max} = 0$ ). The maximal observation horizon is  $N_p^{max} = 10$  and the number of trials for the singularity crossing scheme is  $N_{trials} = 4$ . Initial state of the observer is  $\hat{x}(0) = \text{diag}(0.8, 1.3, 1.3) \cdot x(0)$  and  $\mu_{obs} = 0.8\mu_{model}$ .

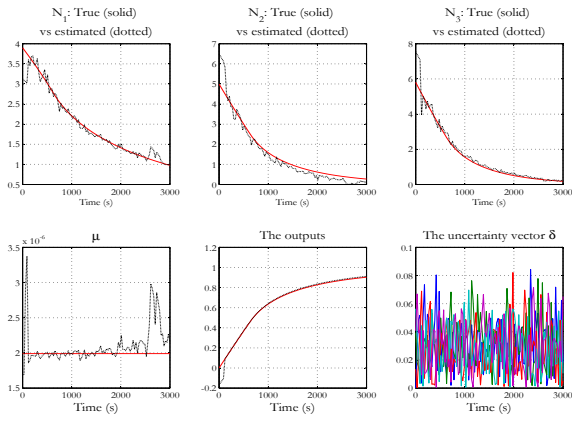


Figure 3: Observer behavior under model uncertainty given by (17)-(21) with  $d_{max} = 10\%$  and in the presence of measurement noise ( $\nu_{max} = 0.01$ ). The maximal observation horizon is  $N_p^{max} = 15$  and the number of trials for the singularity crossing scheme is  $N_{trials} = 4$ . Initial state of the observer is  $\hat{x}(0) = \text{diag}(0.8, 1.3, 1.3) \cdot x(0)$  and  $\mu_{obs} = 0.8\mu_{model}$ . Note that concerning the output, only the true output and the estimated one are shown, measurement noise is not presented. This scenario uses a tolerance  $\varepsilon = 10^{-8}$  for the optimization subroutine.

◇ In order to show the benefit from the singularity crossing mechanism introduced in section 3.1, sim-

ulations with  $N_{trials} = 1$  and  $N_{trials} = 4$  are compared. The results are shown on Figure 4. The scenario being used is the same as the one depicted on figure 3.

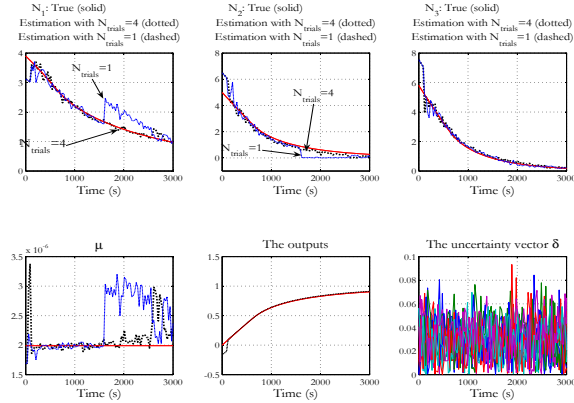


Figure 4: Comparison between the observer behavior when  $N_{trials} = 1$  and  $N_{trials} = 4$  under the scenario depicted on figure 3. Note how the singularity cross mechanism enables to avoid drops in the estimation quality when the observer encounters a singular situation. This scenario uses a tolerance  $\varepsilon = 10^{-8}$  for the optimization subroutine.

◇ **The proposed estimation scheme is real-time implementable**

In order to assess the real-time implementability of the proposed scheme, the computations that lead to the results of figure 3 are given on Figure 5. Note that an explicit upper bound is imposed on the number of function evaluations. More precisely, the internal loop of the optimizer stops as soon as the computation time exceeds the sampling period (30 seconds). Note that all the results shown above use a tolerance threshold  $\varepsilon = 10^{-8}$  for the optimization subroutine. It is shown in the following section illustrating the experimental validation results that this precision is unnecessarily high and quite similar results can be obtained using a lower precision (for instance  $\varepsilon = 10^{-3}$ ) while reducing dramatically the computation time (see figures 6 and 7 hereafter). This is especially true under the multiple trials technique proposed above.

**4.2 Experimental validation**

In this section, the ability of the proposed state observer to reconstruct the individual values of  $N_1$ ,  $N_2$  and  $N_3$  as well as the unmeasured and dynamically unmodeled variable  $\mu$  is shown. Note that in order to experimentally measure the values of the  $N_i$ 's, Samples are withdrawn during the reaction and an inhibitor is added to stop the reaction. The latex is then diluted in a solvent

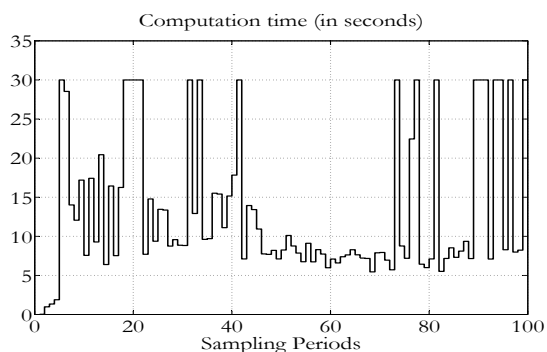


Figure 5: Computation times needed to achieve the state estimation depicted on figure 3. Note that an explicit upper bound has been imposed in the internal loop of the optimizer in order to deliver the best estimation that can be obtained within the available computation time defined by the sampling period (30 seconds). This scenario uses a tolerance  $\varepsilon = 10^{-8}$  for the optimization subroutine.

and injected in a gas chromatograph to measure the residual amount of monomer. By doing so, the true values of the  $N_i$  can be obtained. This has been done only during the 80 first minutes of the Batch where only 9 samples have been analyzed. The dots (\*) on figures 6 and 7 indicate the corresponding measurements.

These figures clearly show the efficiency of the proposed pair (model,observer) in retrieving with an astonishing precision the values of the  $N_i$ 's despite the unmodelled dynamic of  $\mu$ . The rather short computation times (less than 5 seconds compared to the computation times obtained under high precision tolerance) underlines how real-time implementability depends on such parameters that are difficult to set a priori. Finally, it is worth underlying that the times needed to perform  $N_{trials} = 10$  (figure 6) is much less than 10 times the mean computation time for  $N_{trials} = 1$ . This strengthens that the proposed singularity cross technique is different from the multiple initial guess technique in the sense that each trials starts from the best result achieved from the previous trial, only the weighting parameter vector  $\bar{q}$  is randomly modified.

---

## 5 Conclusion & future work

---

In this paper, it is shown that nonlinear constrained receding horizon observer can be efficiently used to estimate the individual number of monomers as well as the dynamically unmodelled number of moles of radicals during a batch terpolymerization process. Simulations show that the proposed scheme presents nice robustness properties against model discrepancy while experimental validation demonstrates its practical effectiveness and real-

time implementability. Since the scheme can be used in semi-batch context, future work concerns the use of the proposed scheme in the design of an output feedback control of the quality of the resulting product.

---

## REFERENCES

---

- Aguilar-Lopez, R. and Maya-Yescas, R. (2005). State estimation for nonlinear systems under model uncertainties: a class of sliding-mode observers. *Journal of Process Control*, 15.
- Alvarez, J. and Lopez, T. (1999). Robust dynamic state estimation of nonlinear plants. *AIChE journal*, 45(1).
- BenAmor, S., III, F. D., and McFarlane, R. (2004). Polymer grade transition control using advanced real-time optimization software. *Journal of Process Control*, 14.
- Buruaga, I., Leiza, J., and Asua, J. (2000). Model-based control of emulsion terpolymerization based on calorimetric measurements. *Polymer Reaction Engineering*, 8(1).
- Dimitratos, J., Georgakis, C., El-Asassar, M., and Klein, A. (1989). Dynamic modeling and state estimation for an emulsion copolymerization reactor. *Computer Chemical Engineering*, 13(1/2).
- Dootingh, M., Viel, F., Rakotopara, D., Gauthier, J., and Hobbes, P. (1992). Nonlinear deterministic observer for state estimation: application to a continuous free radical polymerization reactor. *Computers Chemical Engineering*, 16(8).
- Hammouri, H., McKenna, T., and Othman, S. (1999). Applications of nonlinear observers and control: improving productivity and control of free radical solution copolymerization. *Industrial Engineering and Chemistry Research*, 38.
- Kiparissides, C., Seferlis, P., Mourikas, G., and Morris, A. (2002). Online optimization control of molecular weight properties in batch free-radical polymerization reactors. *Industrial Engineering and Chemistry Research*, 41.
- Kozub, D. and Macgregor, J. (1992). State estimation for semi-batch polymerization reactors. *Chemical Engineering Science*, 47(5).
- Michalska, H. and Mayne, D. Q. (1995). Moving horizon observers and observer-based control. *IEEE Trans. on Automatic Control*, 40:995–1006.
- Othman, N., McKenna, T., and Fvotte, G. (2001). Online monitoring of emulsion terpolymerization processes. *Polymer Reaction Engineering*, 9(4).



- Press, W. H., Teukolsky, S. A., Vetterling, W. T., and Flannery, B. P. (1992). *Numerical Recipes in C. The art of scientific computing. (Second Edition)*. Cambridge University Press.
- Scali, C., Morretta, M., and Semino, D. (1997). Control of the quality of polymer products in continuous reactors: comparison of performance of state estimators with and without updating of parameters. *Journal of Process Control*, 7(5).
- Soroush, M. (1997). Nonlinear state-observer design with application to reactors. *Chemical Engineering Science*, 52(3).
- Tatiraju, S., Soroush, M., and Ogunnaike, B. (1999). Multirate nonlinear state estimation with application to a polymerization reactor. *AIChE Journal*, 45(4).
- Urretabizkain, A., Leiza, J., and Asua, J. (1994). On-line terpolymer composition control in semicontinuous emulsion polymerization. *AIChE Journal*, 40(11).
- Wang, Z., Pla, F., and Corriou, J. (1995). Nonlinear adaptive control of batch styrene polymerization. *Chemical engineering Science*, 50(13).

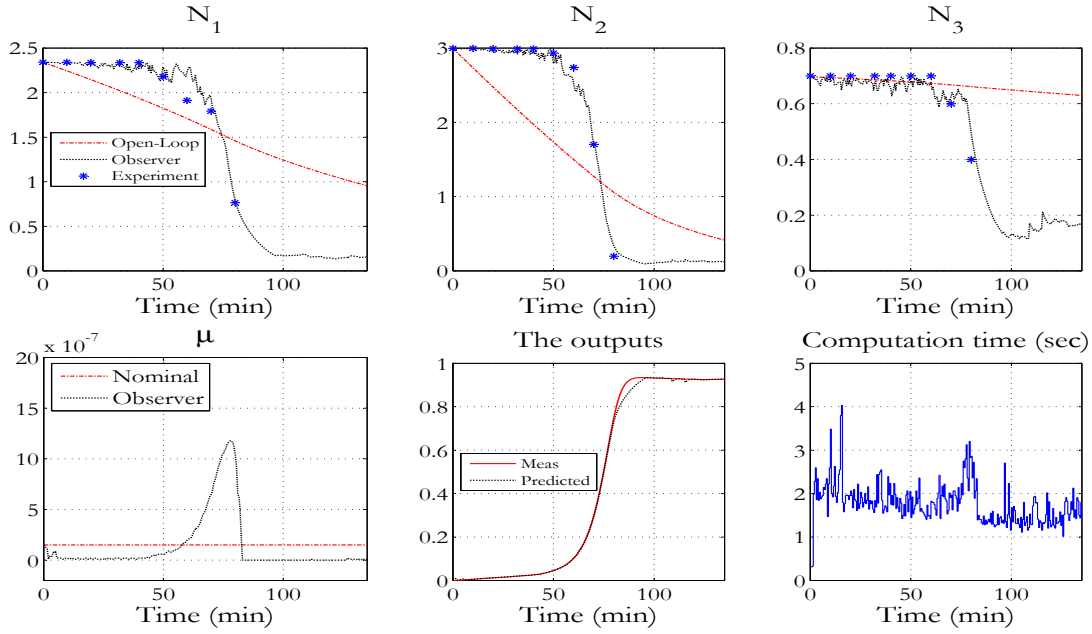


Figure 6: Experimental validation with  $N_{trials} = 10$  and tolerance threshold  $\varepsilon = 10^{-3}$  for the optimization sub-routine. Note how the dynamic behavior of  $\mu$  is recovered despite the constant behavior assumption used in the receding horizon observer model. The dashed lines show what would be obtained if an open-loop simulator is used to obtain an on-line estimation of the  $N_i$ 's. Note the excellent matching between the experimentally measured values of the  $N_i$ 's and those recovered by the observer. The same scenario is depicted on figure 7 where  $N_{trials} = 1$  is used.

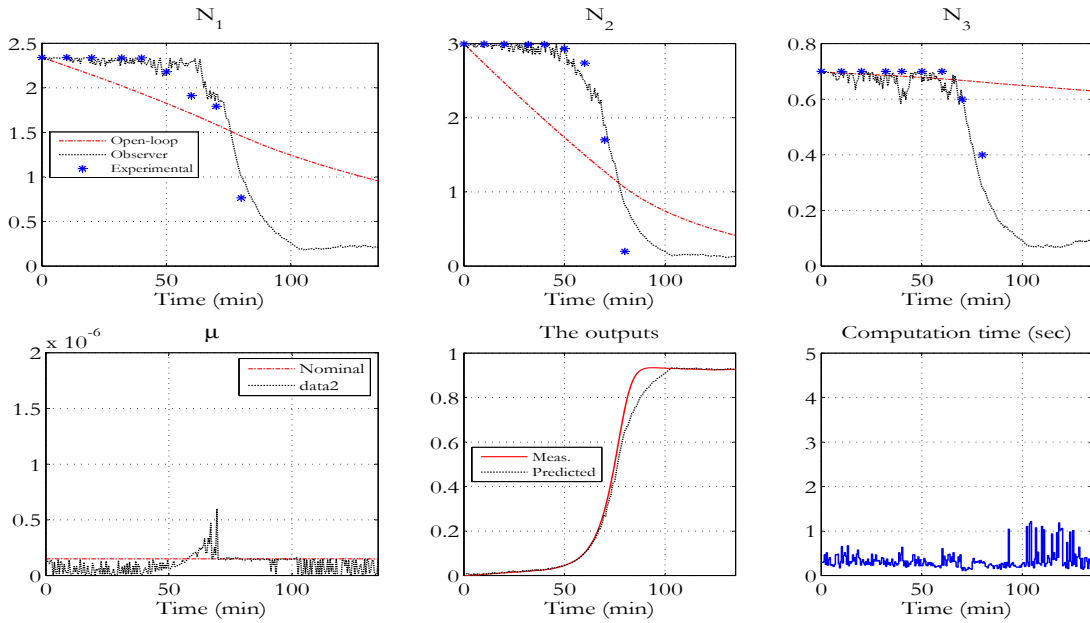


Figure 7: Results under the same experimental validation scenario as figure 6 with  $N_{trials} = 1$  and tolerance threshold  $\varepsilon = 10^{-3}$ . Note the slight drop in the estimation quality (particularly on  $N_2$ ) compared to figure 6 where the singularity cross technique is used.